

# Influence of Surface Treatment on The Mechanical and Viscoelastic Properties of Adhesive Joints Applied to The Oil and Gas Industry

C.E. Moraes<sup>a\*</sup> , L.F.P. Santos<sup>a,b</sup> , T.P.F.G. Leal<sup>c</sup>, E.C. Botelho<sup>b</sup>, M.L. Costa<sup>a,b</sup> 

<sup>a</sup>Universidade Estadual Paulista (UNESP), Faculdade de Engenharia e Ciências, Departamento de Materiais e Tecnologia, Guaratinguetá, SP, Brasil.

<sup>b</sup>Instituto de Pesquisas Tecnológicas (IPT), Laboratório de Estruturas Leves (LEL), Departamento de Materiais Avançados, São José dos Campos, SP, Brasil.

<sup>c</sup>EMBRAER, São José dos Campos, SP, Brasil.

Received: January 10, 2023; Revised: April 12, 2023; Accepted: April 26, 2023

Structural adhesives emerge as an alternative technique for joining materials used in tertiary structures in the oil and gas industry instead of welding, for example, in order to mitigate risks caused by the use of sparks on offshore platforms. Therefore, the present work aims to evaluate the influence of different surface treatments of the adherent material (carbon fiber/epoxy composite) on the mechanical behavior of the adhesive joints through the lap shear test. Furthermore, the viscoelastic properties of the epoxy-based structural adhesive were analyzed via dynamic-mechanical analysis (DMA). The results indicate that the adhesive exhibits residual curing when cured at room temperature and a post-curing process is required to increase its glass transition temperature ( $T_g$ ) and its stiffness. Lap Shear tests results shows that the adherent surface treatment that generated the best mechanical response was cleaning with solvent, despite its lower roughness compared to the fuseply treatment, which indicates a strong correlation between roughness and wettability in obtaining resistant adhesive joints.

**Keywords:** *Structural adhesives, Adhesive joints, Surface treatments, Viscoelastic properties.*

## 1. Introduction

Composites and adhesives materials have been used extensively in several engineering applications including automotive, aerospace, oil and gas and building industries<sup>1-4</sup>. In this context, the use of structural adhesives as a technique for joining materials in the oil and gas industry has as its main strategy the increase of strength/weight ratio allowing a significant reduction in structural weight, better distribution of mechanical stresses by the entire area of the joint and greater corrosion resistance compared to conventional joining techniques, such as welds, screws and rivets<sup>5</sup>. In this sector, structural adhesives are used especially as an alternative to welds, due to some advantages, such as: reduction of operations involving hot work, corrosion protection and time savings<sup>6</sup>. Currently, the use of structural adhesives as a substitute for welds in the oil and gas sector comprises three main situations, namely: (i) composite/composite joints (composite duct connections, saddle supports for non-metallic tubes); (ii) composite/metal joints (repairs of metal pipeline, naval structure and storage tank); (iii) metal/metal joints (saddle supports for metal tubes)<sup>6</sup>. In the literature<sup>7-9</sup>, studies are found indicating the feasibility of using adhesive repairs in composites for two of the most common damages found in floating offshore units: fracture by fatigue and loss of thickness by corrosion<sup>6</sup>. In addition, adhesive joints are also present in secondary and tertiary structures of offshore installations (water ducts, railings, handrails, stairs, vessels, tanks and

light fixtures), being another universe for the application of this material, which the same advantages of increased safety, reduced operating time and the possibility of extending the service life are extremely attractive<sup>10</sup>. Studies<sup>11-18</sup> also present the influence of both the surface preparation in carbon fiber reinforced polymer (CFRP) composites and the thickness of the adhesive layer on the shear strength. Each of these studies points to an adherent surface treatment that promoted better shear resistance, among them through the use of peel plies, sanding with abrasive material and plasma treatment. Regarding the thickness of the adhesive layer, the studies indicated that the increase in this variable was responsible for decreasing the shear strength in single overlap joints. As the term implies, adhesives work through the adhesion process, where two factors are fundamental for it to be effective, wettability and the adhesion method. Wettability is defined as the tendency of a fluid to spread preferentially on a solid surface in the presence of another immiscible phase<sup>19</sup>, that is, it is the ability of an adhesive to maintain close contact with the surfaces to be joined, and good wettability is a key factor in achieving maximum adhesion. As the adhesion process is characterized by the union between two distinct components through their surface, the effectiveness of the union is directly proportional to the contact area between adhesive and adherent<sup>19</sup>. The adhesion method is the way in which the adhesive will interact with the adherent surface, and can occur in three different ways: chemical, where the adhesive and the adherents form chemical bonds between each

\*e-mail: [eduardo.moraes@unesp.br](mailto:eduardo.moraes@unesp.br)

other; mechanical, where the adhesive fills the imperfections (void spaces, pores, surface irregularities, among others) of the adherent surface, promoting a mechanical anchorage between the components; and diffusion or adsorption, where the adhesive diffuses into the adherent at the molecular level<sup>19</sup>. In order to obtain a good structural adhesive bond, there are some aspects involved in achieving intimate molecular contact at the adhesive/adherent interface<sup>20,21</sup>. Achieving such interfacial contact is invariably a necessary first stage in forming a strong and stable adhesive joints<sup>22</sup>. Intrinsic adhesion forces must be strong and effective to ensure that the interface does not act as a weak link in the joint. In this context, the study of the failure mechanism is important to better understand such aspects involved in the adherent/adhesive interface and how mechanical stresses act on such interface<sup>20,22</sup>. For the cases of adhesive joints of fiber-reinforced polymeric materials, the failure mechanisms are defined through the ASTM D5573 (2012) standard. The possible failure modes of this type of material are: (i) Thin layer cohesive failure represents a failure similar to cohesive failure, but in this case the failure occurs very close to the adhesive-adherent interface, characterized by a thin layer of adhesive on a one of the substrate surfaces and another thicker layer of adhesive on the other substrate surface; (ii) Fiber breakage failure, characterized by the breakage of the reinforcing fibers of adherent material; (iii) Matrix failure, characterized by the failure of the substrate, but close to the region of union between the adhesive and the substrate; and (iv) Light fiber breakage failure, characterized by fiber breakage occurring very close to the adhesive-adherent interface, forming a thin layer of reinforcing fibers on the surface of the adhesive. It is worth mentioning that there are also failures resulting from the combination of two or more of the four classes of failure modes represented<sup>23,24</sup>.

In this study, bonded joints of carbon fiber/epoxy composites with epoxy-based structural adhesive were evaluated using the lap shear test. The influences on such mechanical property caused by three types of surface treatments were evaluated, being them, surface cleaned with solvent (isopropyl alcohol), surface sanded with abrasive sponge, and surface with peel ply (Fuseply) application. Also, the influence of the thickness, 0.5 and 1.0 mm, of the adhesive layer were evaluated. The viscoelastic properties of the adhesive were also evaluated through dynamic-mechanical analysis (DMA) and the influences of the post curing process on such properties.

## 2. Materials and Experimental Methods

### 2.1. Materials

The epoxy-based structural adhesive used in this study was supplied by Solvay, AeroPaste X1003, which consists of a paste-like adhesive consisting of two parts: resin and hardener, to be mixed in a 2:1 ratio, respectively. The carbon fiber/epoxy laminates were supplied by Embraer. For the laminates intended for lap shear tests, 12 prepreg layers of 8552 AS4 material were used, where each layer has a thickness of 0.21 mm. The laminates were cured at a temperature of 180 °C and pressure of 100 psi, with final dimensions of (500 x 300 x 2.5) mm. For laminates that

use peel ply as a surface treatment, a polyamide 6-based fabric was placed on the surface of the laminate, and cured together with the composite, leaving a woven impression on the surface, generating a rough pattern, ensuring the roughness of the laminate.

### 2.2. Adhesive viscoelastic characterization

Dynamic-mechanical analysis (DMA) were carried out in order to better understand the adhesive curing process, in addition to its viscoelastic and thermal properties related to this process. For this, adhesive bulk specimens were manufactured in a silicone mold, with dimensions of (47.76 x 13.79 x 1.77) mm. The dynamic mechanical behavior of the specimens was evaluated by a Thermal Analyzer SII Exstar 6000, model DMS 6100, operating in the dual cantilever mode. The experimental conditions used were: temperature range of 25 - 300 °C, heating rate of 3 °C/min, frequency of 1 Hz, and amplitude of 10 µm. Before starting each experiment, the equipment was stabilized at 25 °C by 5 min.

### 2.3. Adherent surface treatments

Adherent surfaces were initially cleaned with neutral detergent, in order to remove any types of contaminants that would not allow the formation of a well-consolidated adhesive/adherent interface, impairing the adhesive bond. After this procedure, surface treatments were carried out on the adherent material as it follows: (i) Cleaning with solvent (isopropyl alcohol), applying unidirectionally with the aid of a clean and intact tissue, taking care not to apply the same region of the tissue twice, avoiding possible recontaminations; (ii) Manual sanding with an abrasive sponge, in the directions +45°, -45°, +90°, -90° and 0°. After that, any particulate residue from sanding was removed using isopropyl alcohol and a clean, intact tissue, taking care not to apply the same region of tissue twice, avoiding possible recontamination; (iii) Surface with application of peel ply (Fuseply), where a fabric based on polyamide-6 is placed against the surface of the laminate before its consolidation and, after that, it is removed leaving a woven impression on the adherent surface, guaranteeing a certain roughness. For this particular surface treatment, no type of cleaning was performed, since the adherent surface is ready for the bonding right after removing the peel ply.

### 2.4. Roughness analysis

Roughness analyzes were carried out on the adherent surfaces in order to verify changes in the roughness parameters caused by the different surface treatments performed, using an untreated surface as a reference. To analyze the topographic characteristics of the adherent surfaces, a 3D analysis was performed using a LEICA DCM 3D optical metrology system, with a 5x confocal objective and blue LED for 405nm. For each surface treatment, 5 measurements were performed and the measured parameters were: (i) Mean roughness ( $R_a$ ), defined as the arithmetic mean of the absolute values of the spacing ordinates ( $y_i$ ), of the points of the surface roughness with reference to the midline, within the measurement path ( $l_m$ ); (ii) Mean square roughness ( $R_q$ ), defined as the square root of the mean squares of the effective profile ordinates in relation to the mean line within the measurement path;

(iii) Maximum roughness height ( $R_z$ ), defined as the vertical distance between the highest peak and the deepest valley within the total evaluation length; (iv) Maximum profile valley depth ( $R_v$ ), which represents the maximum valley height of a profile within the total assessment length in relation to the midline; and (v) Maximum Mean Profile Height ( $R_m$ ), which represents the sum of the maximum peak height and the maximum valley depth of a profile within the reference length<sup>25</sup>.

### 2.5. Bonding process and lap shear specimens

The specimens for the lap shear test were marked on the carbon fiber/epoxy laminates supplied by Embraer in the dimensions of (101.6 x 25.4 x 2.5) mm. After marking, laminates were cutted into groups of 5 specimens, destined to each condition tested. After this procedure, the adhesive AeroPaste X1003 from Solvay was firstly mixed in a proportion of 2 parts of epoxy resin and 1 part of hardener, and then it was applied to the delimited overlap area (12.7 x 25.4 mm) using a non-adherent film. Two different thicknesses of the adhesive layer (0.5 and 1.0 mm) were tested out and, in order to guarantee these thicknesses, supports made in a 3D printer were applied in the disposal areas of the laminates prior to the pressure application with clamps for 24 hours. After the bonding process, the groups of specimens were placed in an oven at 80 °C for 1 hour, for the post-curing process. Specimens were individually cutted after that in a machine with a diamond disk for better finishing of the edge regions.

### 2.6. Lap shear test

Lap Shear tests were performed on a Shimadzu machine, model AG-X, with a load cell of 50 kN and a test speed of 13 mm/min, in accordance with ASTM D5868 and ASTM D1002 standards. For each surface condition and adhesive layer thickness, five specimens were tested. After each test, the fractured surfaces were preserved for fractographic analysis. Shear strength was calculated using force (N) by overlap area (mm<sup>2</sup>) ratio.

### 2.7. Fractographic analysis

In order to evaluate the failure mode of the bonded joints after each test, analyzes by scanning electron microscopy (SEM) were performed. Post-failure adhesive bonds were characterized by scanning electron microscopy, using a Zeiss EVO LS15 model, using the LV-SEM (low voltage scanning

electron microscopy) technique, low voltage and high vacuum, without the need for metallization of the samples.

## 3. Results and Discussions

### 3.1. Dynamic-mechanical analysis

The DMA analyzes were performed in order to evaluate the viscoelastic behavior of the adhesive, as well as the possible influences caused by the post-curing process at 80 °C for 1 hour. Figure 1 illustrates the differences in the storage modulus ( $E'$ ), loss modulus ( $E''$ ) and  $\tan \delta$  curves between the adhesive after curing at room temperature for 24 hours and after the post-curing process at 80 °C for 1 hour, respectively. After curing at room temperature for 24 hours (Figure 1a), it is possible to verify that, at temperatures close to 45 °C, the storage modulus curve shows a decrease, related to the partial glass transition temperature ( $T_g$ ) of the adhesive<sup>26</sup>, that is, the  $T_g$  related to the part of the material that was cured at room temperature. From  $\tan \delta$  curve, this partial  $T_g$  has a value of 60 °C. With the increase in temperature, it is noted that, around 78 °C, the storage modulus increases, a fact related to the beginning of the post-curing process<sup>26</sup>, temperature that corroborates with the choice of 80 °C as being ideal for this process to be carried out. After reaching complete cure at a temperature close to 160 °C, the material reaches its complete rigidity, with no further variation in modulus values, and consequently, in  $\tan \delta$ . After the post curing process of 80 °C for 1 hour (Figure 1b), it can be noticed through the curves of  $E'$ ,  $E''$  and  $\tan \delta$ , no other thermal event related to the post-cure process was evidenced, indicating that complete cure was achieved<sup>26,27</sup>. In addition, the increase in the material's storage modulus at room temperature and the shift of the  $T_g$  to higher values (around 115 °C) indicates an increase in the density of crosslinks caused by the complete curing of the adhesive<sup>26,27</sup>. Table 1 summarizes the results obtained for each condition tested.

### 3.2. Roughness analysis

Table 2 summarizes the roughness information obtained through five measurements for each adherent surface treatment analyzed. Through the data, it can be seen that cleaning with solvent did not cause a significant change in roughness, from a statistical point of view, considering the standard deviation. The decrease of the parameter's values, however, may be

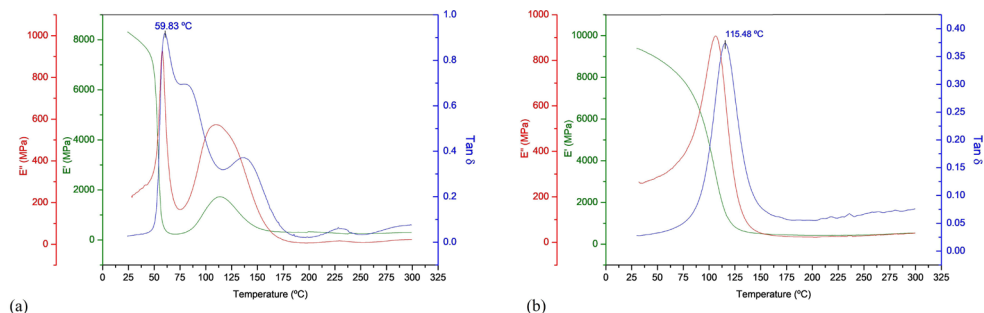


**Figure 1.** Dynamic-mechanical behavior of the adhesive: (a) curing process at room temperature; (b) after post curing process of 80 °C for 1 hour.

related to the analyzed area of the adherent surface, which could slightly change the values since the surface of the laminate material already has a roughness related to the components and manufacturing process used<sup>19,21</sup>. Figure 2a and Figure 2b shows that there are not a significant difference between the surface topography of the untreated surface and the surface cleaned with solvent, in fact, they appear to be quite similar, which indicates that the treatment with solvent did not change the roughness of the adherent surface. Solvent cleaning is an important step though, removing possible contaminants from

the adherent surface that could impair the intimate contact between adhesive and adherent<sup>22</sup>. Regarding to sanding the adherent surface with abrasive sponge, it can be noticed a slightly decrease of the analyzed parameters, which could be related to the removal of a thin surface layer of resin, making the surface less rough. Therefore, the adherent surface has fewer regions of irregularities where the adhesive would be able to fill in such irregularities, impairing the mechanical adhesion when compared to the cleaning with solvent treatment<sup>19,21</sup>. Figure 2c illustrates this difference, indicating a topography of a less rough surface when compared to the two previously analyzed surfaces. With regard to the use of peel ply (Fuseply), it can be seen that this condition was the one that generated the roughest surface, significantly increasing the roughness values when compared to the other treatments. The higher roughness indicates that there are regions of greater irregularities, allowing the adhesive to fill in these irregularities through capillary action, increasing the intimate contact and, consequently, the mechanical adhesion<sup>19,21,25</sup>. In fact, Figure 2d clearly shows the greater irregularities of the adherent surface when compared to the other treatments, generating the best surface condition, in terms of the adherent material roughness, before the bonding process.

**Table 1.** Summary of results obtained by DMA.

	Adhesive cured at room temperature	Adhesive after post-curing process (80 °C / 1 hour)
T <sub>g</sub> (tan δ)	60 °C	116 °C
E' (30 °C)	8.13 GPa	9.38 GPa
E'' (30 °C)	0.25 GPa	0.26 GPa
Tan δ (T <sub>g</sub> )	0.9166	0.3739

**Table 2.** Summary of roughness values obtained from microscopy analysis.

Types of surfaces	Roughness Values				
	R <sub>a</sub> (μm)	R <sub>q</sub> (μm)	R <sub>t</sub> (μm)	R <sub>v</sub> (μm)	R <sub>z</sub> (μm)
<b>Untreated surface</b>	5.8	7.2	24.7	17.6	10.5
	2.5	3.0	11.9	5.5	8.2
	2.3	2.7	10.8	4.8	9.1
	3.6	4.5	18.3	10.8	14.9
	2.5	3.1	12.5	5.7	9.9
<b>Average</b>	<b>3.3 ± 1.4</b>	<b>4.1 ± 1.9</b>	<b>15.6 ± 5.8</b>	<b>8.9 ± 5.5</b>	<b>10.5 ± 2.6</b>
<b>Cleaning with solvent</b>	4.1	4.6	14.1	7.8	14.1
	2.5	3.1	11.0	7.0	10.9
	2.6	3.3	13.3	8.1	9.1
	3.3	3.7	11.5	6.5	9.5
	2.3	2.9	11.6	7.8	11.6
<b>Average</b>	<b>3.0 ± 0.7</b>	<b>3.5 ± 0.7</b>	<b>12.3 ± 1.3</b>	<b>7.5 ± 0.6</b>	<b>11.1 ± 2.0</b>
<b>Sanding with abrasive sponge</b>	3.5	4.3	18.9	10.7	15.1
	2.4	3.0	15.1	7.9	11.4
	1.6	2.0	9.5	4.5	5.4
	1.7	2.0	8.2	4.2	4.5
	3.6	4.6	20.3	11.5	15.2
<b>Average</b>	<b>2.6 ± 0.9</b>	<b>3.2 ± 1.2</b>	<b>14.4 ± 5.4</b>	<b>7.7 ± 3.4</b>	<b>10.3 ± 5.1</b>
<b>Fuseply</b>	8.6	10.6	50.3	24.2	39.5
	10.1	12.1	53.5	25.0	52.3
	8.7	10.8	64.9	35.5	40.9
	9.3	11.7	55.8	23.4	53.5
	11.4	13.5	56.1	25.0	47.4
<b>Average</b>	<b>9.6 ± 1.2</b>	<b>11.7 ± 1.1</b>	<b>56.1 ± 5.4</b>	<b>26.6 ± 4.9</b>	<b>46.7 ± 6.4</b>

**Table 3.** Maximum failure strength for each condition analyzed.

Sample	Fuseply 0.5 mm	Fuseply 1.0 mm	Sanding	Sanding	Cleaning with solvent 0.5 mm	Cleaning with solvent 1.0 mm
			(abrasive sponge) 0.5 mm	(abrasive sponge) 1.0 mm		
Maximum shear strength (MPa)						
1	13.27	13.01	20.83	18.71	24.59	18.80
2	14.99	12.46	25.04	18.31	29.72	22.41
3	11.46	14.56	23.78	16.78	34.71	16.02
4	11.82	7.48	23.12	21.32	28.77	28.22
5	13.03	7.24	30.78	24.14	23.38	31.80
<b>Average</b>	12.91 ± 1.39	10.95 ± 3.37	24.71 ± 3.72	19.85 ± 2.90	28.23 ± 4.51	23.45 ± 6.53
<b>Failure mode</b>	Adhesive	Adhesive	Cohesive	Cohesive	Cohesive	Cohesive

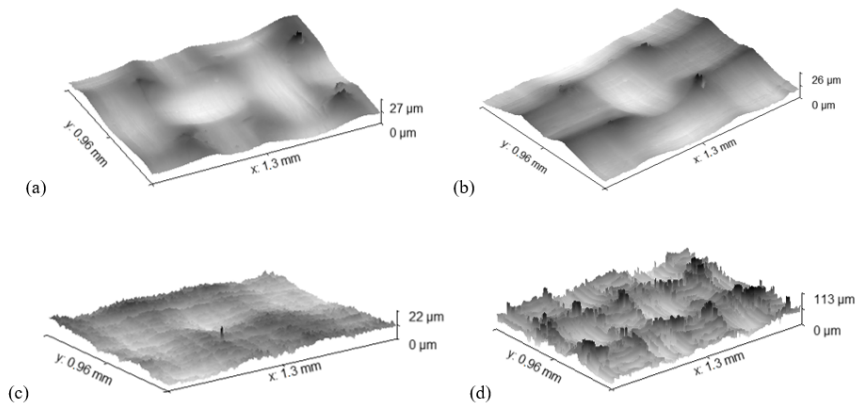


**Figure 2.** Surface mapping: (a) untreated; (b) Cleaning whit solvent; (c) Sanding with abrasive sponge; (d) Fuseply.

### 3.3. Lap shear strength

The lap shear test is widely used to characterize shear strength of adhesive joints, which is extremely important to determine the final application of the joint<sup>28,29</sup>. The maximum shear strength, average values and failure mode of each surface treatment tested are summarized in Table 3. To facilitate understanding and comparison among all the surface treatments, the compiled data is in Figure 3. The load-displacement curves with maximum load indicated for each condition are shown in Figure 4.

Analyzing the results regarding the Fuseply application, it can be seen that there is variation in the maximum shear strength, especially in the condition with adhesive layer thickness of 1.0 mm. In this condition, two specimens presented maximum load significantly lower than the others, indicating possible presence of stress concentrators that affected the mechanical behavior of the samples, causing premature failure of the adhesive joint. In the load-displacement curves for this particular surface treatment (Figure 4a and 4b) it can be noticed a lower level of energy required for the adhesive joint failure to occur when comparing with the other treatments analyzed, indicating poor adhesion<sup>30,31</sup>. This result does not follow what was expected only through roughness analysis of the adherent surfaces, where it was expected that the best mechanical behavior would be the condition using the Fuseply<sup>30</sup>. This occurs due to the type of adhesive used, which is a pasty adhesive with high viscosity and, consequently, low

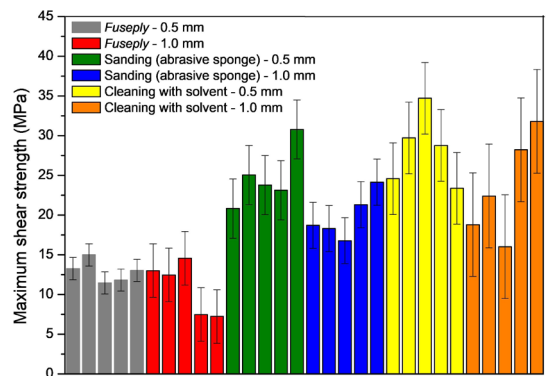


**Figure 3.** Shear strength behavior of the specimens with different surfaces conditions and adhesive layer thickness.

wettability on the adherent surface<sup>32,33</sup>. The low wettability of the adhesive did not allow a proper filling of surface irregularities in the condition that uses Fuseply as a surface treatment, producing low interfacial contact regions and, therefore, lower mechanical adhesion. This hypothesis is reinforced by the result obtained in the sanded treatment. Removing a thin layer of resin from the adherent produced a less rough surface, which enabled the adhesive to fill in the surface irregularities in a better way compared to the fuseply surface treatment<sup>31,33</sup>. The load-displacement curves for the

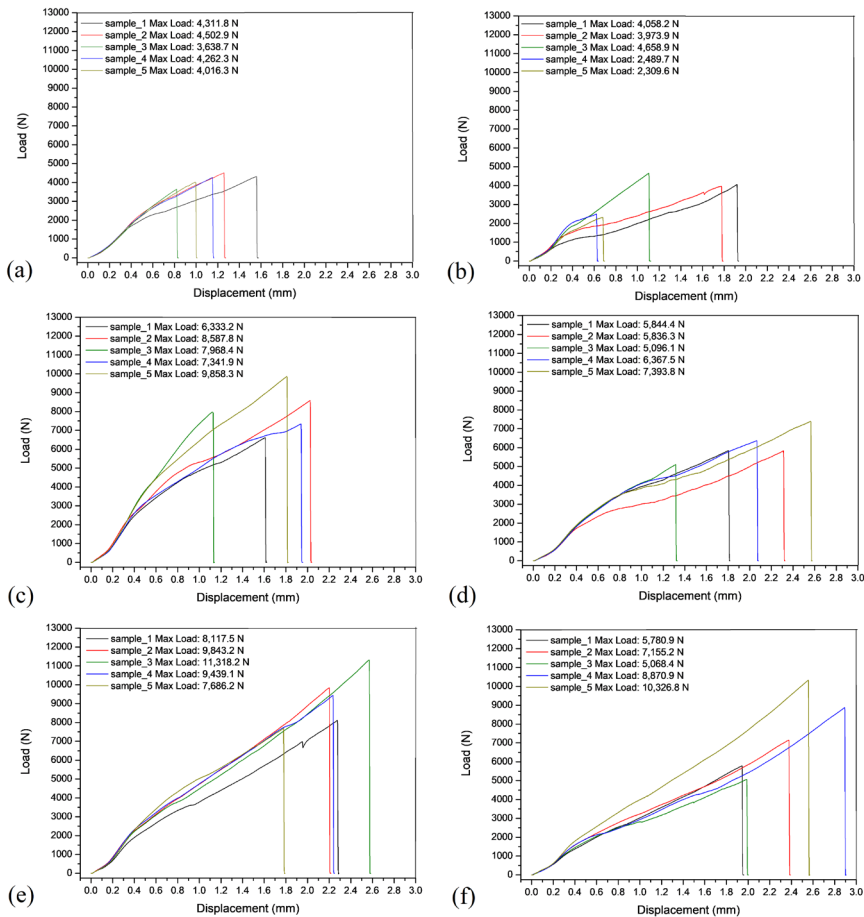


**Figure 4.** Load (N) versus Displacement (mm) curves for: (a) Fuseply – 0.5 mm; (b) Fuseply – 1.0 mm; (c) sanding with abrasive sponge – 0.5 mm; (d) sanding with abrasive sponge – 1.0 mm; (e) Cleaning with solvent – 0.5 mm; (f) Cleaning with solvent – 1.0 mm.

sanding treatment (Figure 4c and 4d) indicated an increase in the levels of energy required for the adhesive joint failure to occur, which indicates an increase in the adhesion efficiency when the surface irregularities are shallower for a pasty adhesive, allowing a better contact between surface-adhesive and, therefore, promoting an increase in the shear strength<sup>19,22</sup>. The surface cleaned with solvent also indicates that the sanding process is not necessary for this particular adhesive, in order to create a strong adhesive joint, promoting a higher shear resistance when compared to the sanded specimen's results. It can be verified by the load-displacement curves for the solvent cleaning surface treatment (Figure 4e and 4f) that the energy levels required for the adhesive joint to failure were higher when comparing with the sanded treatment. This indicates that the surface roughness of the composite itself is already enough in order to obtain a strong joint in terms of shear strength, and the sanding process is not necessary for this particular adhesive used. Regarding the thickness of the adhesive layer, the results indicates that a lower thickness of the adhesive layer is better for shear strength, and an increase in thickness generates greater mobility of the adhesive bond and therefore lower shear strength and premature failure<sup>34,35</sup>. Furthermore, an increase in thickness can lead to greater

formation of voids and defects in the area of the adhesive, thus reducing shear strength<sup>34-36</sup>.

### 3.4. Fractographic analysis

#### 3.4.1. Macroscopic analysis

Figures 5 and 6 illustrates the fracture surfaces for specimens with the different surface treatments tested and with 0.5 mm and 1.0 mm of adhesive layer thickness, respectively. The macroscopic observation is later proved in the section 3.4.2 by the microscopic analysis. For the cleaning with solvent condition (Figure 5a and 6a), it is possible to observe that the failure was due to the cohesive mode for both adhesive thicknesses, with layers of the adhesive on both surfaces of the adherent<sup>5,11,20,30</sup>. Through the roughness measurements of this particular condition, the parameter's values were quite close to those obtained in the sanding with abrasive sponge condition, however, the treatment with solvent and adhesive thickness of 0.5 mm was the one that presented the higher shear resistance ( $28.23 \pm 4.51$  MPa) in general. This can be explained by the presence of a larger layer of adherent resin, acting as one more component in the interaction with the adhesive

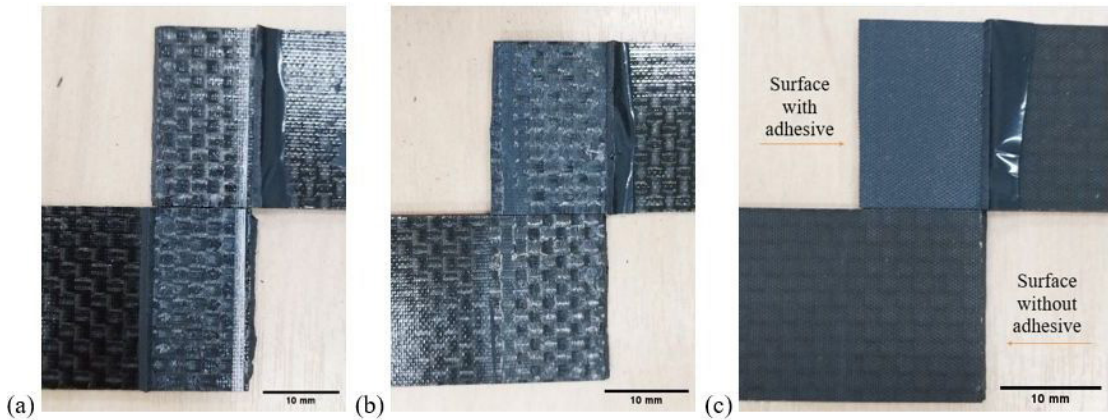


**Figure 5.** Macroscopic view of the failure region of the specimens with 0.5 mm of adhesive layer thickness and following surface treatments: (a) cleaning with solvent; (b) sanding with abrasive sponge; (c) Fuseply application.

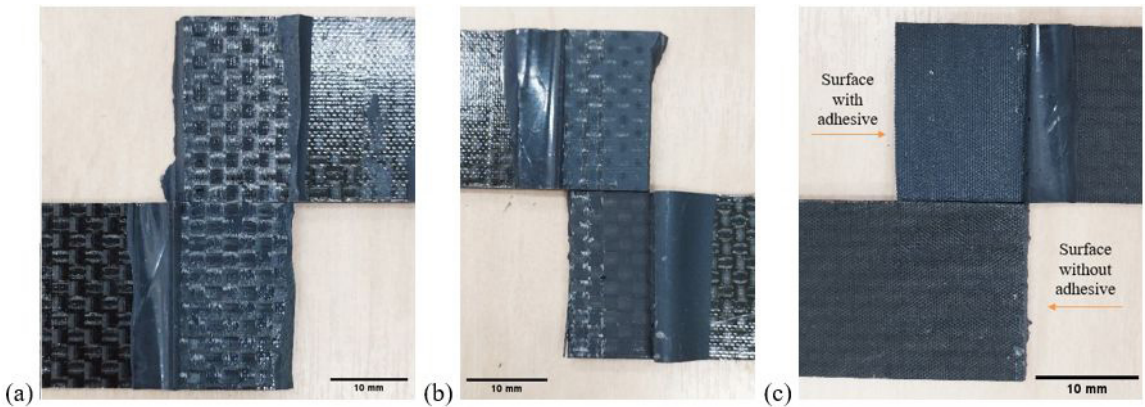


**Figure 6.** Macroscopic view of the failure region of the specimens with 1.0 mm of adhesive layer thickness and following surface treatments: (a) cleaning with solvent; (b) sanding with abrasive sponge; (c) Fuseply application.

and, consequently, increasing the bondable surface area and, therefore, improving mechanical adhesion<sup>30</sup>. Regarding the sanding with abrasive sponge condition (Figure 5b and 6b), it is noted that the failure was due to the cohesive mode for both adhesive thicknesses, with an adhesive layer on both surfaces of the adherent<sup>5,11,20,30</sup>. In this particular case, the adhesive was able to fill in the adherent surface irregularities, forming a well-consolidated adhesive/adherent interface region, presenting a lower shear strength only when compared to the solvent cleaning condition, given the greater interaction area of the adhesive with the adherent<sup>30</sup>. For the Fuseply condition (Figure 5c and 6c), it can be seen that the failure mode was due to adhesive failure for both adhesive thicknesses, which indicates a weak interaction between the adhesive and the adherent surface<sup>11,20,30</sup>. Despite the higher surface roughness for this particular surface treatment, the low wettability of the adhesive was an important factor for the lower shear strength values presented. As it is a high viscosity pasty adhesive<sup>31,32</sup>, it was not able to fill the high surface irregularities of the adherent through capillary action, allowing the formation of regions of low interaction between the adhesive and the adherent and, therefore, impairing the

mechanical behavior<sup>19-21</sup>. A greater roughness of the adherent surface is not the only fundamental factor in the preparation of resistant adhesive joints, but rather the combination of good conditions of adherent roughness and wettability of the adhesive<sup>19-21,30</sup>. The increase in thickness did not change the failure mode as shown in Figure 6.

### 3.4.2. Microscopic analysis

Figure 7 presents the micrographs obtained by SEM analysis for the specimens with the different surface treatments tested and with 0.5 mm of adhesive layer thickness. Taking Griffith's theory into account, the crack propagation process involves the formation of new surfaces, which require energy dissipation<sup>19-21</sup>. For the solvent cleaning condition (Figure 7a), in addition to cohesive failure, it is possible to observe some features such as fiber imprints (yellow arrows), cusps (red arrows), and fractured fibers (orange arrows). This indicates that the dissipated energy levels in the formation of these fracture mechanisms were higher when compared with the sanding and peel ply cases, due to a higher interface adherent/adhesive area, which increased the mechanical adhesion

and, therefore, the shear strength<sup>34</sup>. The microscopies indicate that the samples cleaned with solvent (Figure 7a) and sanded (Figure 7b) with abrasive sponge have similar aspects. For the adhesive in question, surface treatments such as sanding or the use of peel ply are unnecessary, as the roughness of the carbon fiber/epoxy laminate is already sufficient to obtain effective and resistant adhesive joints. In addition to cohesive failure, it is possible to observe slight failures in the fibers, as provided for in the ASTM D5573 standard, indicating that the adhesive was able to permeate the surface irregularities of the adherent, promoting intimate contact and a strong adhesive/adherent interface region and, strengthening the resistance of the adhesive joint<sup>19-21</sup>. Analyzing the surface shown in Figure 7a that presented the highest shear strength, it is possible to observe a surface with the presence of more fracture mechanisms as highlighted. These mechanisms require energy to form and propagate, contributing to greater resistance. Regarding the sanding with abrasive sponge condition (Figure 7b), in addition to cohesive failure, it is possible to observe the presence of fiber imprints (orange arrows), expected for fracture regions that require high levels of energy for crack propagation<sup>34,35</sup>. The lower roughness of this surface indicates that, for the pasty adhesive in question, it is easier to penetrate surface irregularities through capillary action and, consequently, increase the bondable area, improving the shear strength

when compared to the results obtained through the use of Fuseply (Figure 7c). Another highlight is the presence of regions with cusps (red arrows), a fracture mechanism that also requires high levels of energy to occur and dissipate, indicating that, for the adhesive in question, a less rough surface compared to the Fuseply surface was better to obtain more resistant joints<sup>35,36</sup>. For the Fuseply condition, the adhesive failure can be explained by the very low permeation level of the adhesive between the carbon fibers of the adherent, which produced low interaction between adhesive and adherent. In fact, it is possible to observe the fibers practically without the presence of adhesive, presenting a smoother appearance with only a few points with adhesive (orange arrows). The increase in the adhesive layer thickness generated similar fracture surfaces, as shown in Figure 8. Regarding the solvent cleaning treatment (Figure 8a), it is possible to see fiber imprints (yellow arrows), cusps (red arrows), and fractured fibers (orange arrows). Sanding with abrasive sponge (Figure 8b) presented fiber imprints (orange arrows) and cusps (red arrows). Fuseply application (Figure 8c) showed fibers with few points with adhesive (orange arrows). The major difference in the shear behavior with the increase in thickness was the increase of mobility of the joint due to the lower modulus of the adhesive and also the higher presence of stress concentrators (voids) that impaired the joint resistance<sup>34-36</sup>.

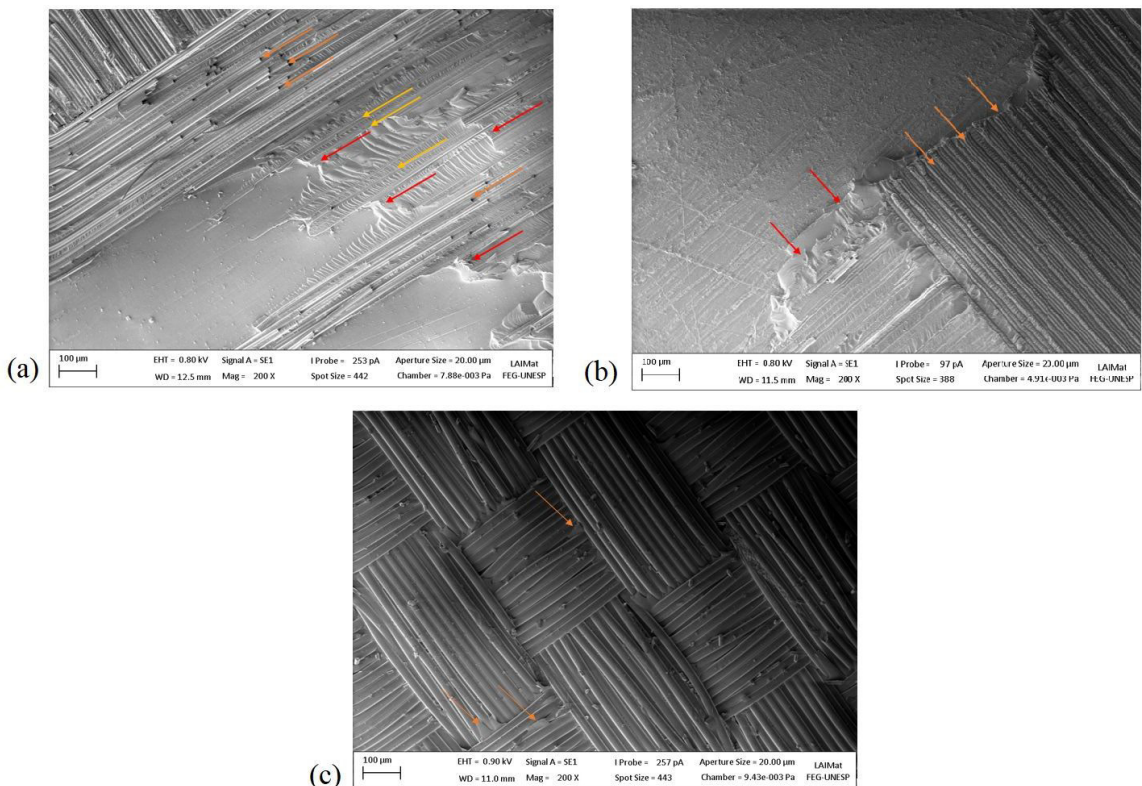


**Figure 7.** Micrographs obtained via SEM of the specimens with 0.5 mm of adhesive layer thickness and following surface treatments: (a) cleaning with solvent (200x); (b) sanding with abrasive sponge (200x); (c) Fuseply application (200x).

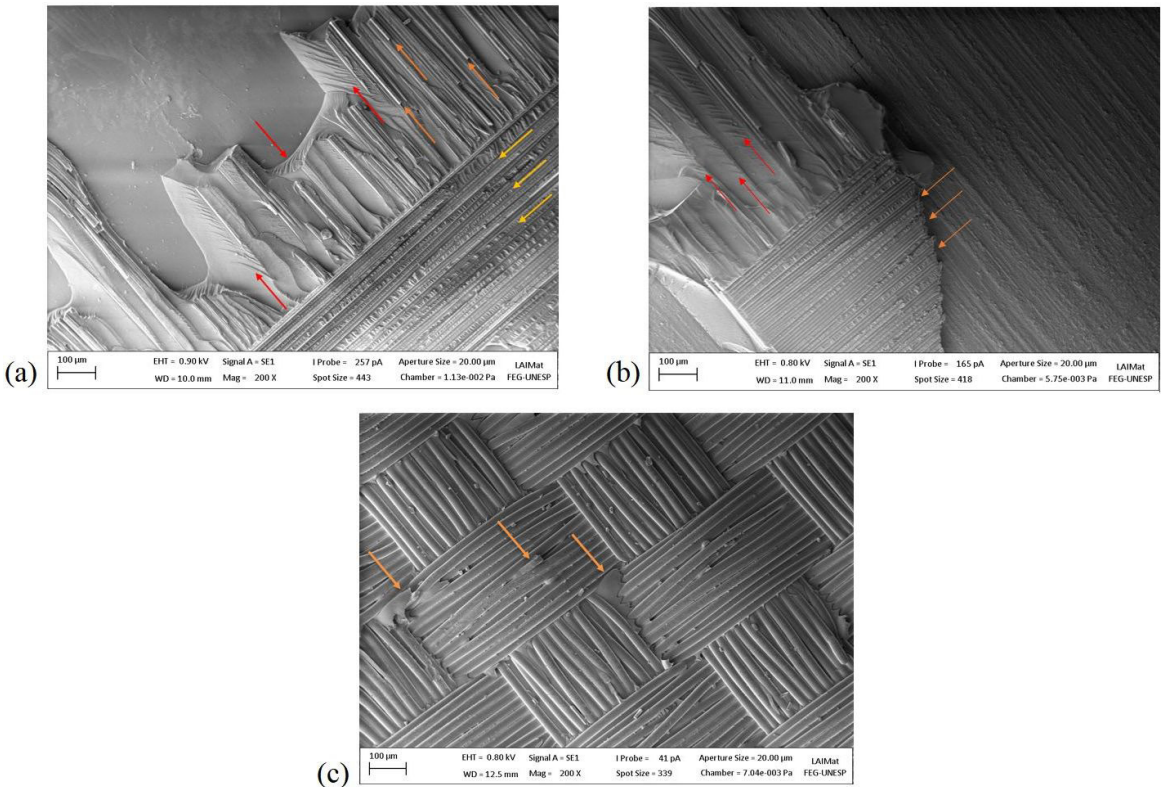


**Figure 8.** Micrographs obtained via SEM of the of the specimens with 1.0 mm of adhesive layer thickness and following surface treatments: (a) cleaning with solvent (200x); (b) sanding with abrasive sponge (200x); (c) Fuseply application (200x).

#### 4. Conclusion

The DMA analyses indicate that the adhesive cured at room temperature does not reach complete cure and a post cure process at 80 °C contributes to the increase of the  $T_g$ , making the adhesive bond more resistant in the thermal scope. Regarding the three adherent surface treatments tested, the one that presented the highest shear strength was the condition of solvent cleaning and the condition that presented the lowest shear strength was the one with Fuseply application. Thus, the low wettability of the adhesive on the adherent surface did not make it possible to fill in the superficial imperfections of the adherent, promoting a low bondable area, reducing the adhesive/adhesive interface region and, therefore, producing a low mechanical adhesion. It is also observed that the increase in thickness impaired the shear strength in all conditions tested, making the adhesive joint more flexible and, therefore, less resistant and more prone to premature failure. For the pasty adhesive studied, this study demonstrated that no treatment of the adherent surface is required beyond the cleaning with solvent for possible contaminants removal, which is an advantage for its use in the oil and gas industry.

#### 5. Acknowledgments

The present work was carried out with the support of the Coordination for the Improvement of Higher Education

Personnel - Brazil (CAPES) - Financing Code 001. The authors are grateful for the financial support from ANP, FINEP and MCTI, through the PRH 34.1, and to CNPq (304876/2020-8 and 306576/2020-1.). The authors would also thank Solvay for supplying the adhesive, Embraer for supplying the laminates and Prof. Dr. Luis Rogério Hein, responsible for the Materials Imaging Laboratory (LAImat) of the Faculty of Engineering and Sciences of Guaratinguetá.

#### 6. References

1. Botelho EC, Nogueira CL, Rezende MC. Monitoring of nylon 6,6/ carbon fiber composites processing by X-ray diffraction and thermal analysis. *J Appl Polym Sci.* 2002;86(12):3114-9.
2. Botelho EC, Scherbakoff N, Rezende MC. Porosity control in glassy carbon by rheological study of the furfuryl resin. *Carbon.* 2001
3. Botelho EC, Almeida RS, Pardini LC, Rezende MC. Influence of hydrothermal conditioning on the elastic properties of Carall laminates. *Appl Compos Mater.* 2007;14(3):209-22.
4. Barbosa LCM, Souza SBD, Botelho EC, Candido GM, Rezende MC. Fractographic evaluation of welded joints of PPS/glass fiber thermoplastic composites. *Eng Fail Anal.* 2019;102:60-8. <http://dx.doi.org/10.1016/j.engfailanal.2019.04.032>.
5. Monsef AS, Renart J, Carreras L, Maimí P, Turon A. Effect of environmental conditioning on pure mode I fracture behavior of adhesively bonded joints. *Theor Appl Fract Mech.* 2020;110:102826. <http://dx.doi.org/10.1016/j.tafmec.2020.102826>.
6. Silva LFM, Öchsner A, Adams RD. Handbook of adhesion technology. 2nd ed. Berlin: Springer; 2008. 1805 p.

7. Mally TS, Johnston AL, Chann M, Walker RH, Keller MW. Performance of a carbon-fiber/epoxy composite for the underwater repair of pressure equipment. *Compos Struct.* 2013;100:542-7. <http://dx.doi.org/10.1016/j.compstruct.2012.12.015>.
8. Osnes H, McGeorge D. Experimental and analytical strength analysis of double-lap joints for marine applications. *Compos, Part B Eng.* 2009;40(1):29-40. <http://dx.doi.org/10.1016/j.compositesb.2008.07.002>.
9. Mattos CHS, Reis JML, Paim LM, Silva ML, Amorim FC, Perrut VA. Analysis of a glass fiber reinforced polyurethane composite repair system for corroded pipelines at elevated temperatures. *Compos Struct.* 2014;114:117-123. <http://dx.doi.org/10.1016/j.compstruct.2014.04.015>.
10. Razavi Setvati M, Mustafa Z, Shafiq N, Syed ZI. A review on composite materials for offshore structures. In: 33rd International Conference on Ocean, Offshore and Arctic Engineering. Proceedings. San Francisco: ASME; 2014. <https://doi.org/10.1115/OMAE2014-23542>
11. Kupski J, Freitas ST, Zarouchas D, Camanho PP, Benedictus R. Composite layup effect on the failure mechanism of single lap bonded joints. *Compos Struct.* 2019;217:14-26. <http://dx.doi.org/10.1016/j.compstruct.2019.02.093>.
12. Yang G, Yang T, Yuan W, Du Y. The influence of surface treatment on the tensile properties of carbon fiber-reinforced epoxy composites-bonded joints. *Compos, Part B Eng.* 2019;160:446-56. <http://dx.doi.org/10.1016/j.compositesb.2018.12.095>.
13. Solvay. FM® 300-2 film adhesive: technical data sheet. Alpharetta: Solvay SA; 2017.
14. Thäslér T, Holtmannspötter J, Gudladt HJ. Surface topography influences on the fatigue behavior of composite joints. In: Hausmann JM, editor. 22nd Symposium on Composites. Zurich: Trans Tech Publications, Ltd; 2019. p. 341-6.
15. Silva AS No, Cruz DTL, Ávila AF. Nano-modified adhesive by graphene: the single lap joint case. *Mater Res.* 2013;16(3):592-6. <http://dx.doi.org/10.1590/S1516-14392013005000022>.
16. Akpınar IA, Gültekin K, Akpınar S, Akbulut H, Ozel A. Research on strength of nanocomposite adhesively bonded composite joints. *Compos, Part B Eng.* 2017;126:143-52. <http://dx.doi.org/10.1016/j.compositesb.2017.06.016>.
17. Sun L, Li C, Tie Y, Hou Y, Duan Y. Experimental and numerical investigations of adhesively bonded CFRP single lap joints subjected to tensile loads. *Int J Adhes Adhes.* 2019;95:102402. <http://dx.doi.org/10.1016/j.ijadhadh.2019.102402>.
18. Jarry E, Shenoi A. Performance of butt strap joints for marine applications. *Int J Adhes Adhes.* 2006;26(3):162-76. <http://dx.doi.org/10.1016/j.ijadhadh.2005.01.010>.
19. Cognard P. Handbook of adhesives and sealants: basic concepts and high tech bonding. 1st ed. Versailles: Elsevier Science; 2005.
20. Kinloch AJ. Adhesion and adhesives: science and technology. 1st ed. London: Chapman and Hall; 1987.
21. Adams RD. Adhesive bonding: science, technology and applications. 2nd ed. Cambridge: Woodhead Publishing; 2021.
22. Ebnesaajad S. Surface treatment of materials for adhesive bonding. 2nd ed. Norwich: William Andrew Publishing; 2014.
23. Wei X, Shen H, Wang H. Fracture failure prediction for composite adhesively bonded double lap joints by an experiment-based approach. *Int J Adhes Adhes.* 2022;114:103110. <http://dx.doi.org/10.1016/j.ijadhadh.2022.103110>.
24. Borsellino C, Urso S, Alderucci T, Chiappini G, Rossi M, Munafò P. Temperature effects on failure mode of double lap glass-aluminum and glass-GFRP joints with epoxy and acrylic adhesive. *Int J Adhes Adhes.* 2021;105:102788. <http://dx.doi.org/10.1016/j.ijadhadh.2020.102788>.
25. Keshavarzi S, Entezari A, Maghsoudi K, Momen G, Jafari R. Ice nucleation on silicone rubber surfaces differing in roughness parameters and wettability: experimental investigation and machine learning-based predictions. *Cold Reg Sci Technol.* 2022;203:103659. <http://dx.doi.org/10.1016/j.coldregions.2022.103659>.
26. Paiva JMF, Mayer S, Cândido GM, Rezende MC. Avaliação da temperatura de transição vítrea de compostos poliméricos reparados de uso aeronáutico. *Polímeros.* 2006;16(1):79-87. <http://dx.doi.org/10.1590/S0104-14282006000100016>.
27. Costa ML, Almeida SFM, Rezende MC. Hygrothermal effects on dynamic mechanical analysis and fracture behavior of polymeric composites. *Mater Res.* 2005;8(3):335-40. <http://dx.doi.org/10.1590/S1516-14392005000300019>.
28. Santos DJ, Carastan DJ, Tavares LB, Batalha GF. Polymeric materials characterization and modeling. In Hashmi S, Batalha GF, Van Tyne CJ, Yilbas BS, editors. *Comprehensive materials processing.* Oxford: Elsevier; 2014. p. 37-63. <http://dx.doi.org/10.1016/B978-0-08-096532-1.00205-3>.
29. Ejaz H, Mubashar A, Uddin E, Ali Z, Arif N. Effect of functionalized and non-functionalized GNPs addition on strength properties of high viscous epoxy adhesive and lap shear joints. *Polym Test.* 2022;113:107680. <http://dx.doi.org/10.1016/j.polymertesting.2022.107680>.
30. Park S, Roy R, Kweon J, Nam Y. Strength and failure modes of surface treated CFRP secondary bonded single lap joints in static and fatigue tensile loading regimes. *Compos, Part A Appl Sci Manuf.* 2020;134:105897. <http://dx.doi.org/10.1016/j.compositesa.2020.105897>.
31. Saleh MN, Saeedifar M, Zarouchas D, Freitas ST. Stress analysis of double-lap bi-material joints bonded with thick adhesive. *Int J Adhes Adhes.* 2020;97:102480. <http://dx.doi.org/10.1016/j.ijadhadh.2019.102480>.
32. Solvay. EF0321 Part A epoxy resin: chemical product safety data sheet. Alpharetta: Solvay SA; 2021.
33. Solvay. EF0321 Part B hardener: chemical product safety data sheet. Alpharetta: Solvay SA; 2021.
34. Shishesaz M, Reza A. The effect of viscoelasticity of adhesives on shear stress distribution in a double-lap joint using analytical method. *J Adhes Sci Technol.* 2013;27(20):2233-50. <http://dx.doi.org/10.1080/01694243.2013.769085>.
35. Amaral L, Yao L, Alderliesten R, Benedictus R. The relation between the strain energy release in fatigue and quasistatic crack growth. *Eng Fract Mech.* 2015;145:86-97. <http://dx.doi.org/10.1016/j.engfracmech.2015.07.018>.
36. Greenhalgh ES. Delamination-dominated failures in polymer composites. In: Greenhalgh ES, editor. *Failure analysis and fractography of polymer composites.* Boca Raton: CRC Press; 2009. p. 164-237 (Woodhead Publishing Series in Composites Science and Engineering).